BEAM DIAGNOSTICS FOR THE PROTON THERAPY FACILITY PROSCAN

Rudolf Dölling, Shixiong Lin, Pierre-Andre Duperrex, Gregor Gamma, Boris Keil

Paul Scherrer Institut, Villigen-PSI, Switzerland, CH-5232, rudolf.doelling@psi.ch

The dedicated new medical facility PROSCAN has restarted the treatment of deep seated tumours with proton beams at Gantry 1. The beam lines to the new Gantry 2 for the further development of the spot-scanning technology, as well as to the replacement of the long established OPTIS facility for the treatment of eye melanoma, and to a material irradiation area, are currently being commissioned. An overview of the beam line diagnostics and those of the Gantry 1 is presented, together with an account of their implementation.

I. INTRODUCTION TO PROSCAN

PSI has a long tradition in the exploration and research of radiation therapy with heavy charged particles. Since 1984 over 4800 eye treatments have been performed at the OPTIS facility using a broad 72 MeV proton beam collimated to the tumour's shape. For the larger and deep seated tumours, the so-called discrete spot-scanning technique has been developed at PSI[1,2]. Here, the Bragg peak of a proton "pencil-beam" of 7-8 mm diameter is scanned in 3 dimensions over the tumour. The dose is delivered as a sequence of discrete dose "spots" positioned within a 5 mm 3D-grid inside the treatment volume. With this technique a very inhomogeneous dose distribution can be generated in a single field. The superposition of several fields is then optimized to achieve a desired dose distribution in the tumour and a low dose in the surrounding tissues. By using a gantry with a rotatable beam delivery system the field incidence on the patient can be varied. More than 280 patients have been treated since 1996 at Gantry 1.

With the PROSCAN project[3,4], PSI's proton therapy activities are set to a new base. The new facility consists of a dedicated 250 MeV cyclotron, an energy degrader and beam lines to the following areas: The existing Gantry 1 and a new Gantry 2, both with a scanning beam, a new eye treatment facility OPTIS2 with a fixed horizontal beam, and a beam line for experiments. It will provide reliably stable beams of varying energy throughout the entire year.

At Gantry 1, the two transversal movements of the pencil beam are done with a fast scanning magnet and a patient-table motion respectively[1]. The third dimension (in depth) is done by varying the beam energy just before the treatment location by inserting polyethylene plates in the beam. This range shifter has the disadvantage of spreading the beam by multiple scattering in the plates, yielding less sharply demarcated dose distributions. In the new Gantry 2, the depth is set by adapting the beam energy with a degrader early in the beam line[5]. The degrader consists of a pair of multiple wedges covering an energy setting in the range of 70-238 MeV. A range change of ~5 mm in water (this corresponds to ~1% change in beam-momentum) has to be set within 50 ms (and the laminated beam line magnets have to be set accordingly). Both lateral scans will be done with scanning magnets before the last 90° bending magnet of the gantry. This design will allow a very fast, complete coverage of the tumour, so that multiple rescanning can be undertaken. The dose inhomogeneity caused by movements of the treatment volume during the scanning process is thus lowered. The treatment of tumours is consequently no longer restricted to sites where organ motion is very limited.

The therapy program at Gantry 1 recommenced in February 2007 and the commissioning of the beam lines to OPTIS2 and the experimental area is underway, while Gantry 2 remains under construction. First treatments with OPTIS2 and Gantry 2 are planned for the beginning, respectively end of next year.

The tasks, responsibilities and hardware are clearly separated between the machine control system (MCS), the user control systems (UCS) of each area and the patient safety system (PaSS)[3,6]. The MCS controls the accelerator and beam lines. For each beam energy, a predefined setting of the beam line (a "tune") will be used. Before each treatment room, a so-called "checkpoint" (CP) has been defined, where the beam should comply with specifications on energy, position, direction, emittance and intensity. (The ion optics of the gantry beam lines reproduce an image of the checkpoint at the location of the treatment.) The UCS of an area can ask the MCS to set a tune only if it has acquired "mastership" of the facility. The mastership enables the UCS to open the beam blockers and to perform a treatment based on its own diagnostics. The correct beam delivery is checked by the PaSS using independent diagnostic elements (plus

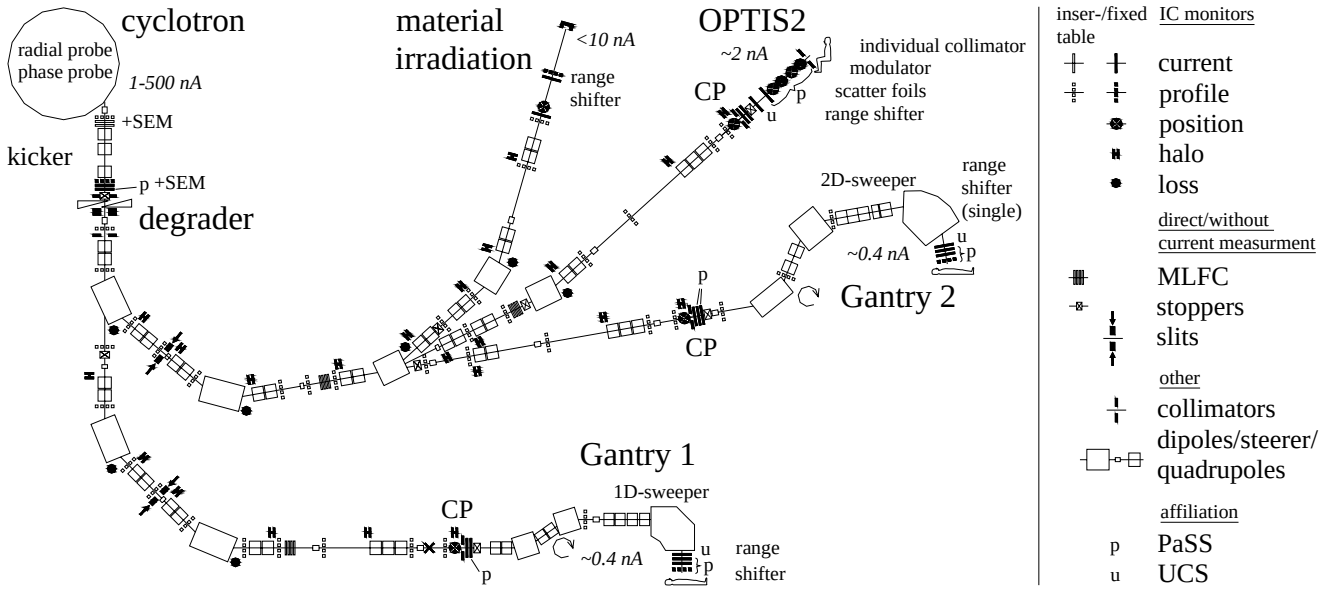

Fig. 1. Overview of the beam diagnostics used or planned at the PROSCAN facility.

dedicated read-back from energy defining elements) for beam line settings (behind the cyclotron and at the checkpoint), beam position and dose delivery (in front of the patient). If outside tolerance, it switches off the beam within a few microseconds.

The beam diagnostics are divided according to the three systems (Fig. 1). Ionization chambers (IC) in several configurations are used as current, profile, position, halo, loss and dose monitors. Using ambient air or nitrogen as chamber gas, sufficient signal is obtained from the small beam currents (0.1 to 500 nA) or its fractions. At the higher currents in front of the degrader, saturation effects can alter the IC signals. Hence, secondary emission monitors have also been added. Thin monitors in the path of the beam are used for continuous beam quality control, while "thick" monitors are inserted in the beam for set-up and tuning purposes only. The beam current can also be measured with Faraday-cup beam stoppers, while beam energy and momentum spread can be determined by multi-leaf faraday cups. An overview on the present diagnostics of the beam lines and Gantry 1 is given in the following. For the diagnostics governed by the MCS, also the read-out electronics as well as the implementation to the MCS and system checks to reach the required high availability are mentioned. The diagnostics under preparation for OPTIS2[7] and Gantry 2 are not discussed.

II. IONIZATION CHAMBER MONITORS

Table 1 gives an overview on the parameters of the IC monitors used. The signal amplification can be calculated from the effective length of the gas volume, contributing to the measurement and the stopping power at the actual proton energy in the chamber gas (at atmospheric pressure).

TABLE I. Parameters of the IC monitors

see chapter	Gap, eff. length, strip pitch [mm]	aper-ture [mm^2]	high vol-tage [kV]	gas	charge collection time [μs]
II.A.1	2, 4, 1 or n/a	62 x 62	2	N_2	12 (e^-:<1)
II.A.2 #1	2.5, 4.9, n/a	Ø12	2	air	18
II.A.2 #2	2.5, 4.9, n/a	Ø32	2	air	18
II.A.3	4, 4, var.	Ø90	0.6	air	160
II.A.4 #1	5, 10, n/a	230x30	2	air	80
II.A.4 #2	10, 20, n/a	230x30	2	air	300
II.A.4 #3	30+10,20,n/a	230x30	3+1.5	N_2	e^-: ~10
II.A.4 #4	20, 20, 4.44	230x60	2	air	1200
II.B.1	n/a, 16, n/a	Ø9	2	air	var.
II.B.2	n/a, 58, n/a	Ø42	2	air	var.
II.B.3	2.5, 5.1, n/a	Ø100	2	air	18
II.B.4	4.5, 9, n/a	Ø82-90	0.3	air	420
II.B.5	10, 100, n/a	200x60	0.3	air	2000

II.A. Parallel-Plane Current and Profile Monitors

The ICs are formed from a stack of alternating high-voltage (HV) and measurement planes which are immersed in the chamber gas and are passed by the beam. Full electrodes provide signals proportional to the beam current and multi-strip electrodes deliver 16 or 32 or more signals for a beam profile. Since the beam line profile monitors use a "1 broader + 14 or 30 regular + 1 broader"-strip pattern, an adequate treatment of the signals of the outer strips at the evaluation of beam center and width is needed[8].

In front of the degrader and at the CPs, current monitors are inserted permanently in the beam. The currents and their ratio are rapidly monitored by the PaSS and are available from the twin-monitors also to the MCS.

II.A.1. Thin Current and Profile Monitors at the Degrader

The permanent monitors in front of the degrader are exposed to the highest beam currents and current densities: up to 1000 nA at beam diameters down to ~2 mm fwqm (full width quarter maximum). To limit saturation effects due to ion recombination, a plane separation of only 2 mm and a high voltage of 2 kV were chosen, well below the practical break-down limit of ~2.5 kV. Nevertheless, the roughly measured saturation effects turned out to be lower than expected from theory[9]. This will be studied in more detail. Titanium foils of 6 μm thickness are used as electrodes to avoid excessive scattering of the beam and to prevent long term radiation damage as expected for Kapton or Mylar foils. The detector is enclosed in a hood with two 50 μm titanium windows. Slow flowing N_2 is used as chamber gas because it is dry and electrochemical migration problems with the isolation gaps on the ceramic foil carriers are prevented thereby[10]. Two current measurements and a horizontal and a vertical profile are available (Fig. 2). Also two high-voltage read-back outputs are available for PaSS and MCS.

Similar but retractable monitors are placed at the exit of the cyclotron. Although they are thin, the scattering of the beam, which is broader at this point, is not negligible.

Fig. 2. Thin monitor. Stack partly disassembled.

II.A.2. Thin Current Monitors at the Checkpoints

At the CPs, the beam is transported through air and the beam current is measured behind collimators of 8 mm (Fig. 3) respectively 30 mm diameter. The current monitors have a small diameter accordingly, resulting in a low sensitivity to microphonic noise (Fig. 4). Although the beam current density at the CPs is low, the plane separation was chosen to be only 2.5 mm in order to keep the charge collection time short. The electrodes are made from 6 μm thick titanium foils[9]. With the FR4 printed-circuit board foil carriers, no electrochemical migration problems occurred when using ambient air as chamber gas and a high voltage of 2 kV.

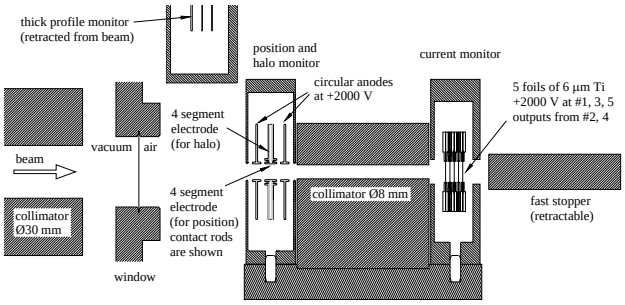

Fig. 3. Schematic view of the CP to Gantry 1 with position and current monitor.

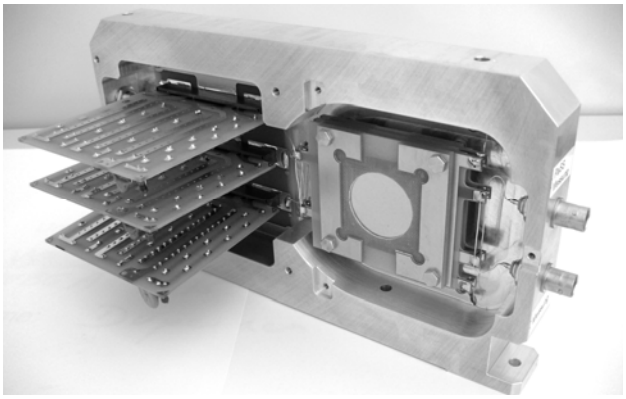

Fig. 4. Current monitor at the CP to OPTIS2 (right) with filters[8] for high-voltage supply and voltage read-back (left).

II.A.3. Insertable Thick Profile Monitors

Insertable multi-strip IC monitors (Fig. 5a), successively introduced into the beam by compressed-air actuators, yield the input information for the calculation of a beam envelope with the "Transport" code[11]. Since these monitors are not thin, only a measurement at one location at a time is possible. A metallised ceramic board[9]

provides 68-strip patterns on both sides for the profiles while two adjacent boards form the high-voltage electrodes. With two exchangeable printed-circuit boards, the signals are combined to 2x 16 or 2x 32 channels. With this arrangement, a strip pitch of 0.5, 1, 1.5, 2, 3 or 4 mm can be chosen[8]. This variability allows for the adaptation of the strip pitch to the expected range of beam profile width, resulting in more accurate width measurements. Microphonic noise was not observed due to the rigid construction. To prevent a patient treatment with a monitor still left in the beam, the rear "window" has been chosen with sufficient thickness to impede beam transmission, thereby triggering an interlock signal from the PaSS transmission verification.

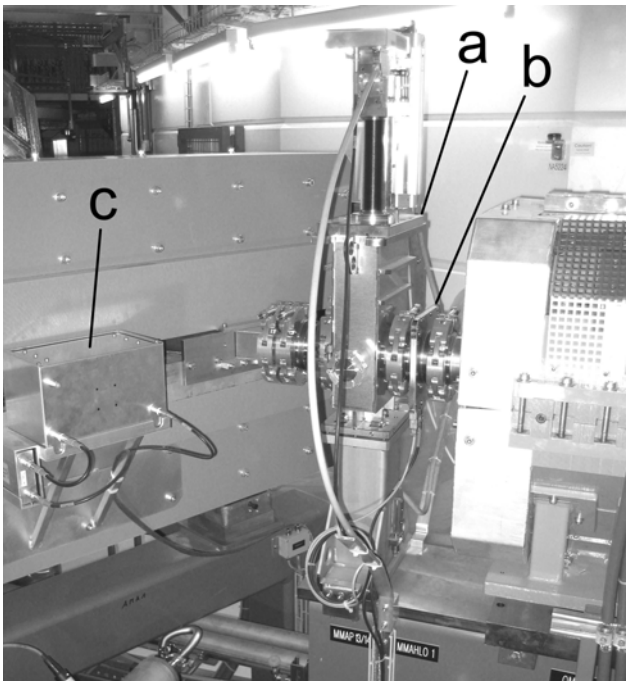

Fig. 5. Thick profile monitor with compressed-air actuator (a). A beam-line halo-monitor is placed at the right bellow (b), and an external loss monitor is seen to the left (c).

II.A.4. Gantry 1 Nozzle Monitors

At Gantry 1, four IC monitors[12] cover the region of the swept beam. The delivery of the dose to the patient is based on the integrated proton flux. Monitor #1, which belongs to the UCS, defines the spot dose and monitor #2 of the PaSS verifies the spot dose after the spot delivery. High gain and stable current to frequency converters have been developed to transfer the IC signal currents into digital pulses. These are fed to their corresponding count-down scalers. When the prescribed spot preset from the monitor 1 system is reached, an interlock signal is sent by the UCS and the fast kicker magnet switches the beam away in less than 50 μs. The PaSS checks the correctness of the beam delivery on a spot by spot basis. Before the spot delivery, two Hall probes (PaSS) in the sweeper and the last bending magnet make indirect beam position checks by measuring the magnetic fields. The resolution is equivalent to about a 1 mm beam shift. Monitor #4, a multi-strip-IC (PaSS), measures the beam position in both transversal directions during the beam spot delivery with a position resolution of about 0.1 mm. The signal sum of monitor #4 is further used for an additional check of the delivered spot dose (PaSS). If the previous spot delivery has been proven to be correct, an interrupt is sent from the PaSS to the UCS in order to initialize the procedure for the application of the next spot. The spot changes are done while the beam is switched off.

The high-voltage planes of monitor #1 and #2 are made of stretched 20 μm Mylar foils, coated double-sided with ~50 nm aluminum, while the central signal plane is a 20 μm aluminum foil. The signal planes of monitor #4 consist of 20 μm thick Kapton foils, coated on one side with a 1 μm thick aluminum strip pattern. Here, the central high-voltage Mylar foil is enclosed by the signal foils. All the detectors are limited by grounded foils.

Monitor #1 and #2 have the drawback of being sensitive to microphonic noise. Therefore, a Frisch-grid IC, monitor #3, was developed[13]. Here, as opposed to the other chambers, the beam travels parallel to the plane electrodes (Fig. 6). Only the electrons which are transmitted through the Frisch grid are collected, giving a fast response of about 10 μs with nitrogen as the chamber gas. This monitor has no detectable microphone effect. However, its gain is less stable than that of the other monitors and depends on the current and the distance of the beam to the Frisch grid. Monitor #3 is used by the PaSS as an additional check of the spot dose.

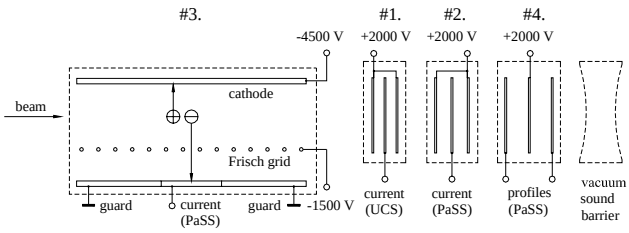

Fig. 6. Nozzle monitors in front of the range shifter.

II.B. Position, Halo and Loss Monitors

In front of the gantries and at the end of the beam lines to the OPTIS2 area and the experimental area, 4-segment IC position monitors have been installed to enable a continuous check of the beam position by the MCS. (Since the output depends also on the beam size, the absolute position can be estimated only roughly, while the beam centering can still be controlled very accurately.) The monitors of the therapy areas have an axisymmetric

electrode configuration and are non-intercepting, thereby avoiding additional beam scattering. They also include a halo-monitor, providing the option of a rough check of the beam diameter.

II.B.1. Position Monitors at the Checkpoints to the Gantries

The non-intercepting position monitor of only 9 mm diameter with an intercepting circumferential 4-segment halo monitor[9] is part of a compact arrangement at the CP to Gantry 1 (Fig. 3). (The intercepted part of the beam is stopped in the following collimator.) The centered beam position can be determined to less than 0.05 mm[10].

II.B.2. Position Monitors at the checkpoint to OPTIS2

A double-scattering technique is foreseen for the beam application at OPTIS2[7] requiring a position monitor[10] with larger aperture than at the gantries. It is provided by the electrode configuration shown in Fig. 7.

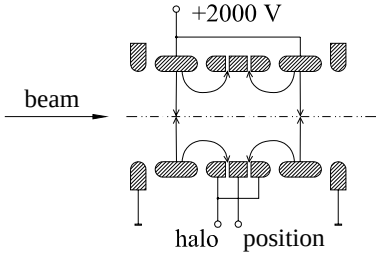

Fig. 7. Position and halo-monitor at the CP to OPTIS2. The separatrices (electric field lines) defining the drainage areas of both are shown.

II.B.3. Position Monitor in Front of the Experimental Area

The parallel-plane IC is made from 12 μm thick, double-sided aluminized Kapton foils[10]. One measurement electrode is segmented into 4 quadrants and a second unsegmented one is used for current measurement.

II.B.4. Halo Monitors in the beam lines

The monitors can be folded around modified bellows adjacent to the quadrupole doublets and triplets where the beam diameter is largest (Fig. 5b). The axisymmetric IC[8] protrudes circumferentially 5 mm into the 90 mm diameter beam pipe giving enough signal to detect traversing beam current fractions of below 1 pA (Fig. 8). This provides a very sensitive loss control and allows an online control of the stability of the beam settings, except for strongly collimated beams.

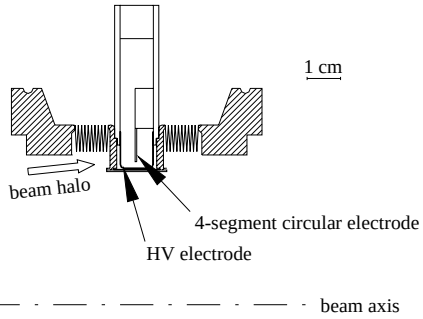

Fig. 8. Halo-monitor. The electrodes are soldered to the printed-circuit boards which form the housing.

II.B.5. External loss Monitors

For the detection of beam losses in the dipole-magnets, standard IC (as operated at PSIs high-current accelerators[14]) with a stack of 11 brass electrodes are placed behind the magnet gaps (Fig. 5c).

III. SECONDARY EMISSION MONITORS

The monitor of Chapter II.A.1 is doubled by the same device, mounted just behind it directly in the vacuum box of the degrader, serving the same clients as secondary emission current and profile monitor. A voltage of 300 V is applied to pull the electrons. The signal amplification (electron yield) is only 0.053, which is approximately 0.1 % of that of the IC. Hence, microphonic noise corresponding to a beam current of up to some tens of nA_{pp} plays a role here[9]. (The voltage will be reduced to 30 V to diminish this effect.) The stability of the secondary emission coefficient of titanium against ageing was one major reason for its choice. Nevertheless, changes of the electron yield of 5 % were observed when shifting the beam across the detector.

IV. MULTI-LEAF FARADAY CUPS (MLFCs)

Two variants of insertable in-vacuum MLFCs are available for fast measurements of the beam energy and momentum spread. Both use the current readings from 64 copper sheets, separated by 75 μm Kapton foils, but use different sets of sheet thicknesses. Both cover the full energy range of the degrader (gantry-MLFC: 68 - 252 MeV, OPTIS2-MLFC: 65 - 255 MeV) but the OPTIS2-MLFC uses the thinnest copper sheets of 0.1 and 0.2 mm to improve the resolution in the range of 65 - 85 MeV. With a refined evaluation[10], an accuracy corresponding to 0.05 mm H_2O can be expected in the range of 65 - 79 MeV for the OPTIS2-MLFC, and of 0.15 to 0.8 mm H_2O for the gantry-MLFC over the full energy range. This has to be verified. A recent comparative measurement with both variants is shown in Fig. 9.

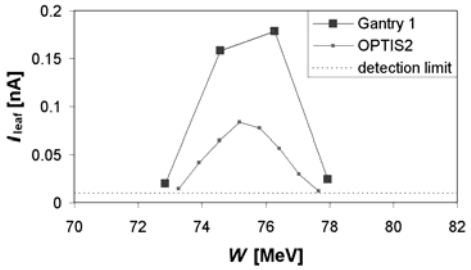

Fig. 9. Beam energy distributions derived from the range distributions measured with both variants of MLFCs at a beam current of 0.46 nA. (A simple evaluation is used. A symbols horizontal position marks the average of the energies corresponding to a leaf. The symbol width corresponds to the accuracy of the position determination expected from the refined treatment.)

V. ELECTRONICS OF MCS-DIAGNOSTICS

All signal currents from the beam lines are measured with logarithmic amplifier modules. The measurement electronics and the high-voltage modules for the detectors are located some 40 meters away outside of the concrete shielding to prevent radiation damage and to allow for service without opening the vault. At the low signal currents, it is imperative to use cables with a low production of microphonic noise and to prevent ground loops. A good electrical shield is also of importance. Several cables have been tested for their susceptibility to microphonic noise and differences of several orders of magnitude were found[8]. Since the HV-supply cables are grounded at both ends, filters are required to prevent the introduction of noise via the high-voltage electrodes[8]. The signal cables are grounded only at the monitor housing.

V.A. Logarithmic Amplifier Modules and Digital Processing Electronics

The signal currents from the monitors are digitized by VMEbus backplane modules ("LogIV modules") that contain logarithmic current-to-voltage converters and ADCs. The ADC data of each module is processed by a VME64x board ("VPC Board") with two FPGAs (Field Programmable Gate Arrays) for digital signal processing and interfacing to the MCS.

V.A.1. LogIV modules

The LogIV modules[15] measure currents between ~10 pA and 10 mA using logarithmic current-to-voltage converters (500 mV/decade). An accuracy of ±2% is aspired in the range of 100 pA to 100 μA. The resulting voltages are synchronously digitized using 4-channel 14-bit ADCs at 5 kSamples/s (up to 50 kSamples/s are possible). One module type (LogIV32) measures 32 current channels whereas the second type (LogIV4x4) measures 4 groups of 4 input currents each. These sensitive electronics are mounted within metallic enclosures for shielding from external electromagnetic noise. To avoid ground loops, the electrical grounds of the transition board and that of the enclosed electronics (being at the machine ground) are separated. For the LogIV4x4 there is a separate ground potential for each group of currents. Also the uncalibrated analog voltages are available as outputs and used by the PaSS beam current measurements.

Logarithmic amplifiers use the logarithmic relationship between emitter voltage and collector current of a transistor. The resulting bandwidth depends on the input current. To measure this dependence either a small sine or a square wave modulation was superimposed to a given input current. For the sine modulation technique, the -3dB frequency was measured, whereas, for the square wave modulation, the rise and fall time have been measured and the corresponding cut-off frequency calculated (Fig. 10). Both methods deliver similar results. However, the square wave modulation is faster and allows for an easier averaging of the measurement data.

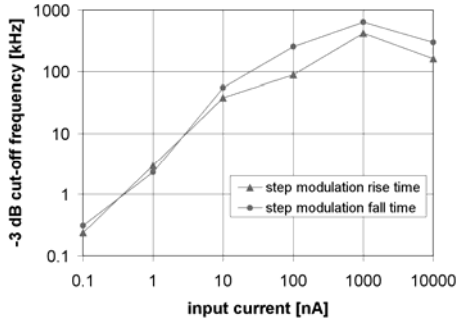

Fig. 10. LogIV dynamic response bandwidth.

V.A.2. VPC board hardware architecture

Fig. 11 shows the main hardware components of the VPC board[16] that was developed at PSI as a generic signal processing back-end for a variety of accelerator diagnostics applications. The core of the VME64x board consists of two Virtex2Pro FPGAs ("System FPGA" and "User FPGA") with two on-chip PowerPC processors each, a floating point DSP, and RAM. The System FPGA contains generic firmware that is common to all applications of the VPC board, like the high-speed (2eSST) VMEbus interface to the accelerator control system or the interface to the compact flash controller that allows in-situ updates of the FPGA firmware (via VMEbus) that is stored on a compact flash card. The User FPGA contains the application-dependent firmware. It can acquire measurement data either from two application-dependent mezzanine modules or, as in the case of PROSCAN, from modules on the VMEbus backplane.

The two optional SFP fibre optic transceivers of the VPC allow for the real-time distribution of measurement data at 2.125 Gbit/s and may be used e.g. for interlock purposes. The external 4 MByte ZBT RAM of the User FPGA is used e.g. to store measurement data waveforms and lookup tables.

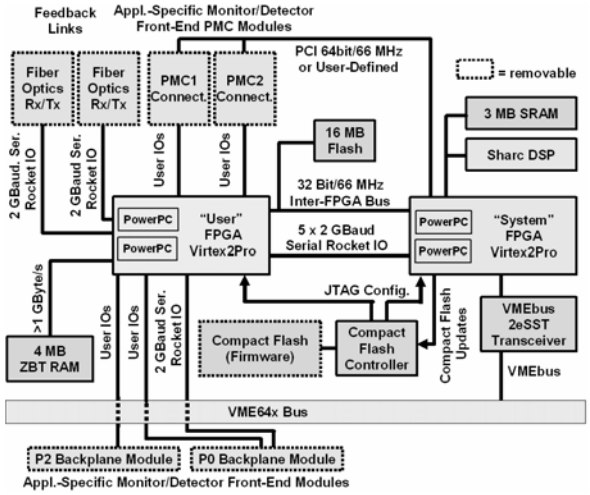

Figure 11: Block diagram of the VPC board.

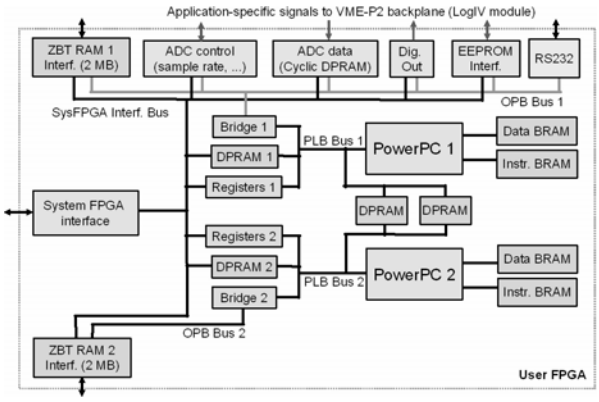

Figure 12: Schematic diagram of the VPC User FPGA firmware for PROSCAN.

V.A.3. VPC FPGA firmware architecture

Fig. 12 shows the architecture of the FPGA firmware in the User FPGA. PowerPC1 receives and processes the ADC data that it receives from the LogIV modules via suitable interface modules connected to the VMEbus backplane I/Os on one side and to the PLB/OPB processor bus on the other side. The PowerPC calibrates (and thereby linearises) the detector currents using lookup tables, calculates a variety of functions like beam size etc., and provides averages, filters, interlocks and ZBT RAM storage of current waveforms, with flexible scope-like trigger features. While the software for PowerPC1 is vital for the operation of the MCS diagnostics at PROSCAN, PowerPC2 is available for any kind of data analysis and its software may be changed frequently without risk for the operation of the accelerator.

Data transfer between each PowerPC and the System FPGA (and thus the VME-based control system) is done by internal dual-ported RAMs ("DPRAM1", "DPRAM2" in Fig. 12), by registers and by the external ZBT RAMs. Dual-ported VHDL interface modules allow full access to internal and external RAMs and VME backplane interfaces both by PowerPC1/PowerPC2 and VMEbus.

V.B. Measurement Options

In addition to the individual signal currents of the attached LogIV board, the VPC-board makes available a variety[17] of parameters calculated from simultaneously sampled signal currents and updated with 5 kHz. These include the current sum, the maximum current; for LogIV32 center position and width of one or two profiles; for LogIV4x4 horizontal and vertical beam positions for halo-monitors, signal current ratios for transmission measurements, signal current differences and signal current integrals. Every signal is doubly available: filtered with two configurable low-pass filters. The same firmware[18] is implemented in both modules by a CompactFlash card.

If a user requests a parameter from the MCS via a specific name, the MCS fetch it from the VPC-board via the VMEbus. Another option is to request, trigger and read out en-bloc a series of "profiles". A "profile" consists of all signal currents of a module, simultaneously sampled and each averaged over the time interval n * 0.2 ms (with n = 1, 2, ... selectable). Up to 4095 "profiles" can be taken with one request. This option allows the simultaneous sampling of beam profiles, which is needed because strong beam current fluctuations from the ion source are present[19].

Under different names, the user can require the MCS to deliver further derived parameters: the beam currents derived from the readings of current, profile or position monitors (by taking into account the energy-dependent conversion factors of the detectors[20]), beam current ratios or beam current integrals. Hence, every profile monitor can be used for a direct display of the beam current at its location.

VI. INTERLOCKS IN THE MCS

To all the individual signal currents and to the parameters derived in the module, limits can be set and the generation of interlocks can be activated via the VMEbus. Also the relevant low-pass filters can be configured[18]. Thereby an ensemble[17] of interlocks becomes available, which can be used for checks of the quality of the beam (current, transmission, position, width, losses) and of the detector systems (high-voltage read-back, consistent output of twin-detectors). The high-voltage

modules give interlocks, if the voltage is too low or the supply current too high, indicating a short-circuit in the detectors or filters. Both modules generate interlocks if the self-tests fail.

Since the beam power is too low to cause damage and the patient's safety is assured by the PaSS, the interlocks in the frame of the MCS are solely a tool for the enhancement of the stability and reproducibility of the beam and of the availability of the diagnostics and possibly of other machine components.

Although possible, interlocks depending on the actual machine tune or user mode, or the fast evaluation of signals arriving distributed to several modules, are not foreseen in the MCS of PROSCAN. Nevertheless these capabilities are provided by the PaSS electronics and will be used also in a next generation of electronics for the diagnostics of PSI's high power proton beam lines.

VII. MCS-DIAGNOSTICS SYSTEM CHECKS

In addition to the permanent supervision of the diagnostics systems by interlocks, periodical tests without beam, using dedicated MCS-routines, are foreseen[8]. These are the check for detector leakage currents by observing the supply currents, and the "influence test" which checks the mechanical integrity of the detector, the presence of the high voltage, the integrity of every signal path and isolation and the readout electronics: The high voltage is switched off and on with defined slopes, thereby capacitively coupling a signal to the measurement electrodes. This response can be compared to previously recorded data. All the detectors including the MLFC (but with the exception of the moving slit current measurement) are prepared for this test.

VIII. CONCLUSIONS

An ensemble of detectors and readout electronics, has been tailored to the needs of the proton therapy at PSI. It is in extensive use for the operation of Gantry 1 and for the commissioning of the new beam lines of the PROSCAN facility.

ACKNOWLEDGMENTS

We like to thank M. Graf and M. Rohrer for the thorough mechanical design and R. Erne, B. Rippstein and R. Widmer for assembling and wiring of the monitors, actuators and vacuum chambers.

REFERENCES

1. E. PEDRONI ET AL., "The 200-MeV proton therapy project at the Paul Scherrer Institute: Conceptual design and practical realization", *Med. Phys.*, **22 (1),** 37-53 (1995).
2. E. PEDRONI ET AL., "Experimental characterization and physical modelling of the dose distribution of scanned proton pencil beams", *Phys. Med. Biol.*, **50,** 541–561 (2005).
3. J. M. SCHIPPERS ET AL., "The use of protons in cancer therapy at PSI and related instrumentation", *Journal of Physics: Conference Series*, **41,** 61–71 (2006).
4. J. M. SCHIPPERS ET AL., "The SC cyclotron and beam lines of PSI's new proton therapy facility PROSCAN", *NIM B*, **261**, 773–776 (2007).
5. E. PEDRONI ET AL., "The PSI Gantry 2: a second generation proton scanning gantry", *Z. Med. Phys.*, **14,** 25–34 (2004).
6. I. JIROUSEK ET AL., "The concept of the PROSCAN patient safety system", *Proc. 9th ICALEPCS*, Gyeongju, 13-17. Oct. 2003, pp. 572-574 (2003).
7. M. J. VAN GOETHEM ET AL. , "Conceptual design of a nozzle for OPTIS2", *PTCOG 44 Meeting*, Zurich, 14-16 June 2006.
8. R. DÖLLING, "Profile, current and halo monitors of the PROSCAN beam lines", *AIP Conf. Proc.*, **732**, 244-252 (2004).
9. R. DÖLLING, "Ionisation chambers and secondary emission monitors at the PROSCAN beam lines", *AIP Conf. Proc.*, **868**, 271-280 (2006).
10. R. DÖLLING, "Progress of the diagnostics at the PROSCAN beam lines", *Proc. DIPAC2007*, Venice, 20-23 May 2007, to be published.
11. U. ROHRER, "*PSI Graphic Transport Framework based on a CERN-SLAC-FERMILAB version by K. L. Brown et al.*"
12. S. LIN ET AL., "Principles and 10 year experience of the beam monitor system at the PSI scanned proton therapy facility", *PTCOG 46 Meeting*, Zibo, Shandong, China, 21-23 May 2007.
13. S. LIN ET AL., "Studies of a grid chamber for fast on line dosimetry", *PSI Scientific Report 1995*, pp. 16-18 (1995).
14. R. DÖLLING ET AL., "Beam diagnostics at the high power proton beam lines and targets at PSI", *Proc. DIPAC2005*, Lyon, 6-8 June 2005, pp. 228-232, JACoW (2005).
15. P.-A DUPERREX ET AL., "Latest diagnostic electronics development for the PROSCAN proton accelerator", AIP Conf. Proc., **732**, 268-275 (2004).
16. B. KEIL ET AL., "The PSI VPC board - first applications of a common digital back-end for electron and proton beam instrumentation at PSI", *Proc. DIPAC2005*, Lyon, 6-8 June 2005, pp. 140-142, JACoW (2005).
17 R. DÖLLING, PROSCAN-document P24/DR84-612
18 B. KEIL, PROSCAN-document P24/KI84-701
19 R. DÖLLING, PROSCAN-document P24/DR84-703
20 R. DÖLLING, PROSCAN-document P24/DR84-620